

**AN EXPERIMENTAL SET-UP FOR MEASUREMENT  
OF THE POWER ABSORBED FROM 900 MHz GSM  
STANDING WAVES BY SMALL ANIMALS,  
ILLUSTRATED BY APPLICATION TO  
PICROTOXIN-TREATED RATS**

**E. Lopez-Martin**

Morphological Sciences Department  
University of Santiago de Compostela  
Santiago de Compostela 15782, Spain

**J. C. Brégains**

Radiating Systems Group  
University of Santiago de Compostela  
Santiago de Compostela 15782, Spain

**F. J. Jorge-Barreiro**

Morphological Sciences Department  
University of Santiago de Compostela  
Santiago de Compostela 15782, Spain

**J. L. Sebastián-Franco**

Applied Physics III Department  
Universidad Complutense of Madrid  
Madrid 2804, Spain

**E. Moreno-Piquero and F. Ares-Pena**

Radiating Systems Group  
University of Santiago de Compostela  
Santiago de Compostela 15782, Spain

**Abstract**—We describe an experimental set-up for exposure of small animals to radiofrequency standing waves that allows direct measurement of the power absorbed by the animal. Essentially, the set-up consists of a metallic box containing an antenna and experimental animal immobilized in a methacrylate holder; a signal generator feeding the antenna; and a power meter. In addition, the box can also contain a video camera to record the animal's behaviour, and a receiving antenna (connected externally to a power meter and a spectrum analyser) to detect undesired (external) radiation and possible harmonics of the radiating system. The absorbed power measurement trivially allows calculation of whole-body mean SAR from the animal's weight; and assuming local SARs to be proportional to whole-body mean SAR, the latter can be used to adjust organ-specific SAR predictions obtained by simulation using a commercial FDTD program with a numerical phantom. The use of the system is illustrated by application to rats given subconvulsive doses of picrotoxin to induce a seizure-prone state analogous to epilepsy: levels of the neuronal activity marker c-Fos in the frontal and piriform cortex of picrotoxin-treated rats exposed to 900 MHz GSM radiation were twice as high as those of unexposed animals.

## 1. INTRODUCTION

Current experimental set-ups for investigation of the effects of mobile communications signals on small animals subject the animals to travelling waves [1–3]. Specific absorption rates (SARs) at given locations in the animal are calculated either from thermal [3–5] or electrical field [5, 6] measurements, or by simulation using a numerical phantom [6, 7]; and whole-body SARs can be calculated by integration of the local SARs.

Indoors, radiation in the high megahertz or low gigahertz bands is present as standing waves [8], and therefore it is reasonable to suggest that could have effects that are qualitatively or quantitatively different from those of travelling waves, due to the different nature of both electromagnetic signals.

Unlike the travelling wave set-ups referred to above, the standing wave apparatus described here allows direct measurement of the power absorbed by the animal. Furthermore, assuming local SARs to be approximately proportional to whole-body mean SAR, this measurement can be used to apply a correction to organ-specific SARs

obtained by simulation using numerical phantoms<sup>†</sup>.

Although the risk of thermally induced pathology deriving from the use of cell phones appears to be minimal if current limits on the power emitted by these devices are respected, the possibility that pathological effects may ensue from direct interference between cell phone radiation and the electrical activity of the central nervous system (CNS) has not been ruled out. On the contrary, it is well-established that the CNS in general [9], and the cerebral cortex in particular [10, 11], is sensitive to radio frequency (RF) radiation. A radiation intensity too low to affect other organs or systems could therefore have significant pathological effects on the CNS [12].

In principle it seems possible that epileptic individuals may be especially sensitive to the effects of RF radiation, given the electrochemical instability of the neuron circuits involved in the cerebral electrical storms responsible for their seizures [9]. In previous work [13], we have in fact shown that radiation of the type used by the Global System for Mobile communications (GSM) triggers seizures in rats in which a seizure-prone state analogous to epilepsy had been induced by subconvulsive doses of picrotoxin [14].

Here we illustrate the use of the new apparatus by partial replication of our earlier study of rats, focusing in particular on neural activity in the piriform cortex and the frontal motor cortex as reflected by levels of the neuronal activation marker *c-Fos* [15, 16].

## 2. MATERIALS AND METHODS

### 2.1. Experimental Set-up and Numerical Phantom

Figure 1 shows the experimental set-up. Essentially, the experimental animal is immobilized in a methacrylate holder that is placed, together with a transmitting antenna, inside a metallic chamber that is large enough to contribute only minimally to the stress on the animal; the chamber currently used is 150 cm long, 70 cm high and 46 cm wide (internal measurements). Optionally, the chamber may also contain a receiving antenna and a video camera. The transmitter is connected

---

<sup>†</sup> It is obvious that local SAR depends much on the characteristics of the organ under consideration, because two animals with the same weight and volume could have different proportions in their internal constitutions, not only including weights and volumes, but electrical parameters as well. Our assumption is made upon the base that these differences are small enough so as the approximate local SAR value obtained is not out of proportion with respect to a realistic one, and its variability could be more or less the one attributed to the relatively small differences that a specific rat has in its internal constitution with respect to an average one of the same (or approximate) weight. It is useful to remember that the numerical model of the rat is considered to be an average sample of a female 198.3 g Sprague-Dawley rat, as specified in the text.

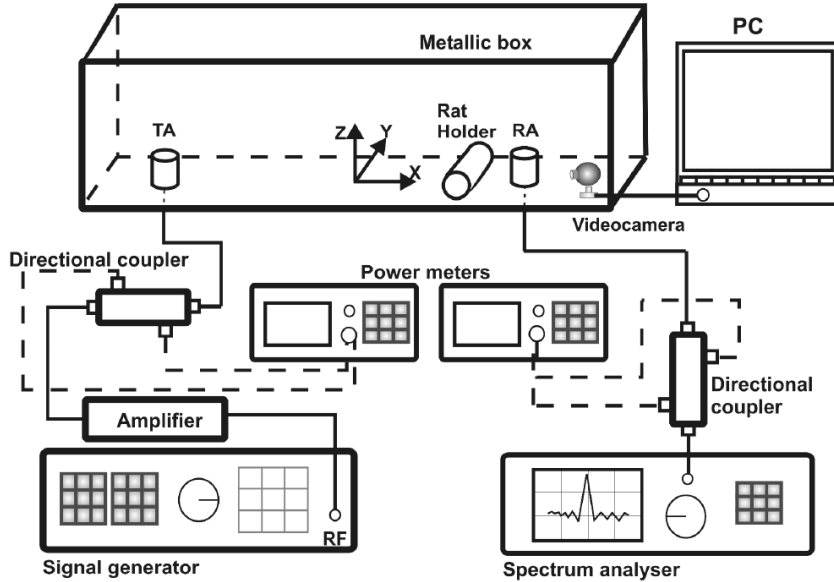


**Figure 1.** Diagram of the experimental set-up. The signal generator, spectrum analyser and power meters are from Agilent (Models E4438C, E4407B and E4418B, respectively), the linear power amplifier from Aethercomm, and the directional couplers from Narda (Model 3282B-30). TA, transmitting antenna; RA, receiving antenna. The origin of coordinates is located at the centre of the floor of the chamber.

to an RF signal generator (via an amplifier) and to a power meter that allows direct measurement of the power dissipated in the chamber; the power absorbed by the animal can then be calculated by difference with respect to measurements taken with the holder in the same position but with no animal inside. The receiving antenna, when used, is connected to a spectrum analyser and a power meter, and can be used to detect and measure undesired (external) radiation and possible harmonics of the radiating system. The videocamera, when used, allows the behaviour of the animal to be recorded.

Figure 2 shows the design of the holder for a young adult rat. With this design, the centre of the rat's brain lies in the terminal cone, approximately on the axis of the holder about 2 cm from the base of the cone.

The positions of the animal holder and receiving antenna (if used) are determined in the light of the field distribution inside the chamber. Figure 3(a) shows the distribution of  $|E|$  in the

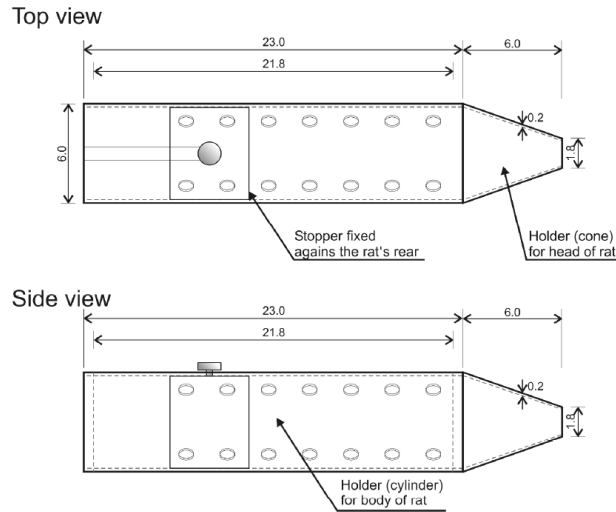


**Figure 2.** The methacrylate rat holder.

vertical longitudinal centreplane as calculated using SPEAG FDTD software [17] to simulate the chamber and transmitting antenna. The chamber walls were modelled as a perfect electrical conductor and the antenna as a  $\lambda/4$  monopole<sup>‡</sup> emitting 900 MHz radiation with GSM-type modulation; the number of three-dimensional cells filling the simulated chamber was approximately 500,000, and the steady state was attained after 400 radiation periods. In this study the standard position of the holder was parallel to the width of the chamber (i.e., in the direction of the  $Y$  axis of Figure 1), with the centre of the rat's brain ideally at  $(X, Y, Z \text{ [cm]}) = (26.0, -3.0, 4.0)$  when the origin of coordinates is located at the centre of the floor of the chamber as in Figure 1. The appropriateness of this location for quasi-uniform radiation of the rat was checked by an analogous simulation of the chamber with both antennas and the rat inside, the rat being modelled by a SPEAG numerical phantom that had been constructed from MRI sections of a 198.3 g male Sprague-Dawley rat taken 1.15 mm apart, and which distinguishes 60 different tissues (SEMCAD model R8; Figure 3(b) shows the distribution of  $|E|$  in a horizontal plane at the level of the phantom's head.

<sup>‡</sup> Although the physical constitution of the experimental model of the antenna was slightly different from a  $\lambda/4$  monopole, its radiation diagram could be considered as being the same than that generated by such a monopole.

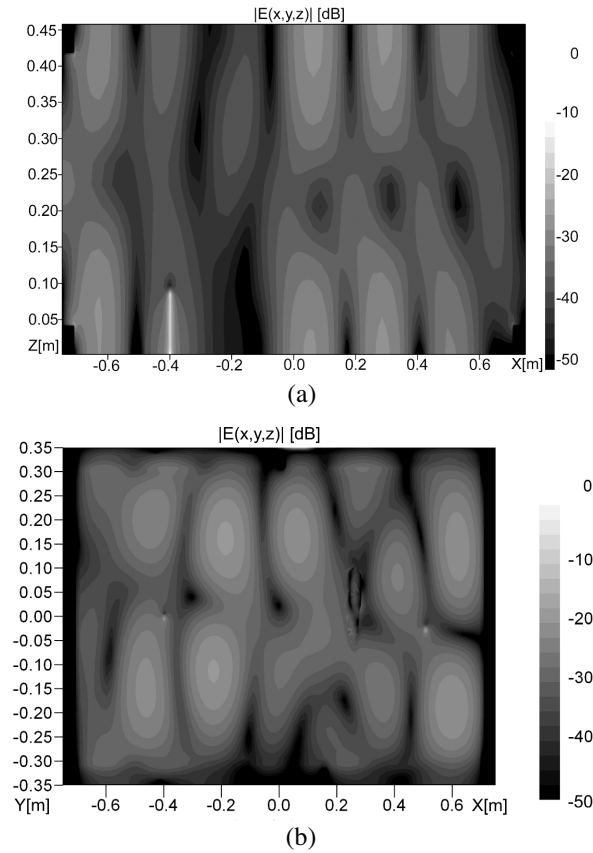


**Figure 3.** (a) SEMCAD-simulated distribution of the  $|E|$  field in the chamber in the plane  $Y = 0$  (see Figure 1 for coordinates) when the chamber only contains a transmitting antenna, modelled as a  $\lambda/4$  monopole. (b) SEMCAD-simulated distribution of  $|E|$  in a horizontal plane at the level of the phantom's head when the chamber contains the phantom and the transmitting and receiving antennas.

## 2.2. Animals, and Experimental Design and Protocols

Thirty-two adult male Sprague-Dawley rats weighing 200–250 g and previously housed under standard conditions (12/12 h light/dark cycle, 22°C), with food and water *ad libitum*, were divided into four groups of eight. Group PR animals were destined for injection of picrotoxin followed by 2 hours' exposure in the radiation chamber to 900 MHz GSM-type radiation, i.e., radiation pulsed with a TDM period of 4615  $\mu\text{s}$  and a slot width of 577  $\mu\text{s}$ ; group PNR for injection of

microtoxin followed by 2 hours' immobilization in the radiation chamber without radiation; group CR for 2 hours' exposure to radiation without prior injection of microtoxin; and group CNR for 2 hours' immobilization in the chamber without radiation or prior injection of microtoxin. Microtoxin, when used, was injected intraperitoneally at the subconvulsive dosage of  $2 \text{ mg Kg}^{-1}$  [13, 14]. In all groups, the animals were used one at a time, and the receiving antenna and video camera were present in the chamber in all experiments. Radiation was emitted at an average power level of 1 W, which lies between the 0.25 W average and the 2 W peak that are typical of cell phone use. The receiving antenna detected harmonics of 1800 and 2700 MHz, but their maximum power levels were respectively 24 and 37 dBm below the 900 MHz signal. The exposure time of 2 h is considered as the usual limit of continuous use of cell phones, and is the time normally employed in acute exposure studies [18].

In an auxiliary experiment constituting a rough check on the validity of the numerical phantom for our rats, six rats with an average weight of 195.5 g (range 192–202 g) were all irradiated as above without injection of microtoxin. In a second auxiliary experiment, carried out to estimate the extent to which errors in rat placement may have affected measurements, a single 202 g rat was placed successively in each of six positions differing from the standard position by a slight translation or rotation, as shown in Figure 4, and in each position was irradiated long enough for measurement of the absorbed power.

All experiments were carried out in accordance with the research protocols established by the Animal Care Committee of the University of Santiago de Compostela.

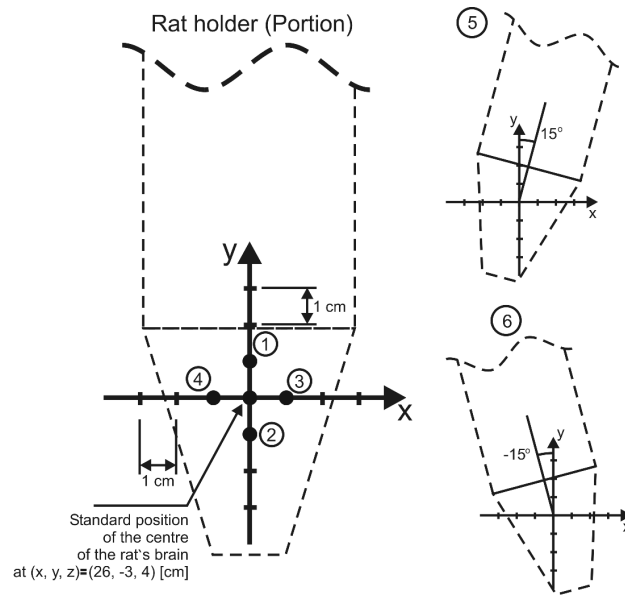
### 2.3. Calculation of Local SARs

Figure 5 shows the distribution of  $|E|$  in a vertical plane approximately through the midline of the rat phantom, as calculated in a simulation in which the rat and antennas were placed in the same positions as in the experiments described above. Figure 6 shows the resulting distribution of local (1-g-averaged) SARs in the same plane.

As noted above, measurement of the actual power absorbed by the experimental rat allows application of a correction factor to local SAR predictions calculated by numerical simulation. Specifically, we calculate an estimated local SAR,  $SAR_E$ , from the expression

$$\begin{aligned} SAR_E &= SAR_S \times (WBMSAR_E)/(WBMSAR_S) \\ &= SAR_S \times (P_E/W_E)/(P_S/W_S) \end{aligned} \quad (1)$$

where  $SAR_S$  is the corresponding simulated SAR,  $WBMSAR_E$  and



**Figure 4.** Positions of the rat holder in the second auxiliary experiment, performed to estimate experimental error due to misplacement. Rotations are about a vertical axis through the position of the centre of the rat's brain in the standard position [(26.0, -3.0, 4.0) cm; see Figure 1 for coordinates].

$WBMSAR_S$  are respectively the experimental and simulated whole-body mean SARs,  $P_E$  and  $P_S$  the corresponding absorbed powers, and  $W_E$  and  $W_S$  the weights of the experimental and simulated rats. We thus assume that local SARs are proportional to whole-body mean SAR, at least over the small weight range employed in the present study, 200–250 g. In any case, in this study SARs were mainly used simply to check that local power absorption was nowhere near sufficient to have thermal effects, so great accuracy in SAR values was unnecessary.

#### 2.4. Histology and Statistical Analysis

After 2 h in the radiation chamber the rats were sacrificed by deep anaesthesia with pentothal and perfusion via the ascending aorta with paraformaldehyde at 4°C. The brain was dissected out and transferred to phosphate buffer of pH 7.4, and 50  $\mu\text{m}$  transverse sections were cut with a vibrotome. Alternate sections were stained with 0.01% toluidin



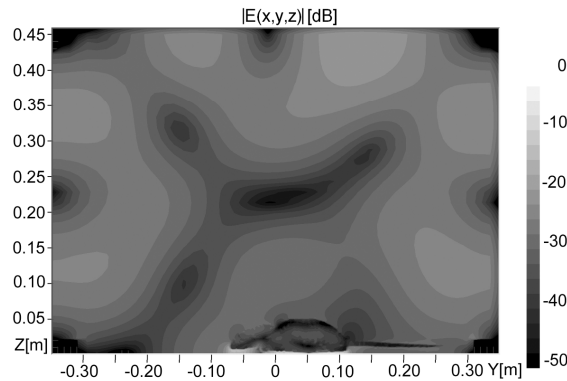


**Figure 5.** SEMCAD-simulated distribution of  $|E|$  in the plane  $X = 0.26$  m (approximately through the midline of the rat; see Figure 1 for coordinates) when the chamber contains the phantom and the transmitting and receiving antennas.

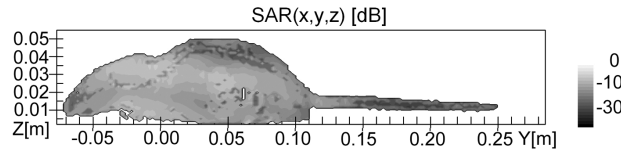


**Figure 6.** Distribution of local SARs in the phantom rat “exposed” to 1 W of 900 MHz GSM radiation, in the plane  $X = 0.26$  m (approximately through the midline of the rat; see Figure 1 for coordinates).

blue in acetate buffer or treated immunohistochemically as follows.

Sections floating freely in phosphate-buffered saline (PBS) were pre-treated for 1 h with normal rabbit serum and Triton X-100 (respectively 10% and 0.25% in 0.02% potassium PBS (KPBS)) and then exposed overnight at room temperature to polyclonal sheep anti-Fos antibody (from Cambridge Research Biochemicals) at a dilution of 1 : 1000 in KPBS. The sections were then rinsed with KPBS; incubated for 1 h with biotinylated rabbit anti-sheep antibody (from Vector) at a dilution of 1 : 500 in KPBS; rinsed thrice with KPBS; incubated for 30 min with an avidin-biotin-peroxidase complex prepared following the instructions of the manufacturer (DAKO); and finally labelled with 3, 3-diaminobenzidine (DAB) in imidazole-HCl-buffered  $H_2O_2$  solution (from DAKO).

In each rat, c-Fos positivity was evaluated in four sections

through each of the two brain areas considered (piriform and frontal motor cortex). In each section, c-Fos-positive cells were counted (by investigators who were blind to exposure conditions) in a  $0.30 \times 0.24$  mm field magnified  $\times 20$  by a Nikon Eclipse E200 microscope connected to a computer running morphometric software from Kappa. Each DAB dot was counted as a c-Fos-positive neuron; counts per field are reported as means  $\pm$  SEMs.

The significance of between-group differences was estimated by two-way analysis of variance (*picrotoxin status* (“treated” or “untreated”)  $\times$  *radiation status* (“irradiated” or “non-irradiated”)) following tests confirming the normality of the statistical distributions and the homogeneity of variance. *Post hoc* comparisons were made using Scheffé-type tests. Differences with  $p < 0.05$  were considered to be statistically significant.

### 3. RESULTS

In the six-rat auxiliary experiment, the average absorbed power per mW of incident power was 0.080 mW (range 0.043–0.115 mW). The corresponding figure for the simulation with the 200 g phantom was 60.76 mW (0.081 mW of absorbed power per mW of incident power), a difference of only 0.8% that supports the validity of the phantom.

In the second auxiliary experiment, the mean relative absolute deviation in absorbed power from the value measured in the standard position,  $(1/6)\sum_{i=1}^6 |P_{Si} - P_{S0}|/P_{S0}$  (where  $P_{Si}$  is the absorbed power in position  $i$  and  $P_{S0}$  the absorbed power in the standard position), was 35.8%. Since the shifts in position used in this experiment were really quite exaggerated, this figure is probably a very conservative overestimate of the real uncertainty deriving from this cause.

Table 1 lists average absorbed power values and SARs in the rats irradiated in the main study, as calculated using Equation (1). All the SARs are well below the threshold of 5 mW/g above which absorbed radiation is likely to result in thermal effects [19, 20]. Note the great similarity between the SAR patterns of the two experimental groups; the difference between the effects of radiation on picrotoxin-treated and untreated rats (see below) cannot be attributed to differences in power absorption.

After 5 minutes' exposure, the irradiated picrotoxin-treated rats (group PR) began to exhibit myoclonic jerks and then suffered intermittent seizures during 20–30 min, whereas non-irradiated picrotoxin-treated rats (group PNR) exhibited bursts of locomotor activity for between 3 and 5 min; in both cases, the animals remained immobile but alert for the remainder of their time in the radiation

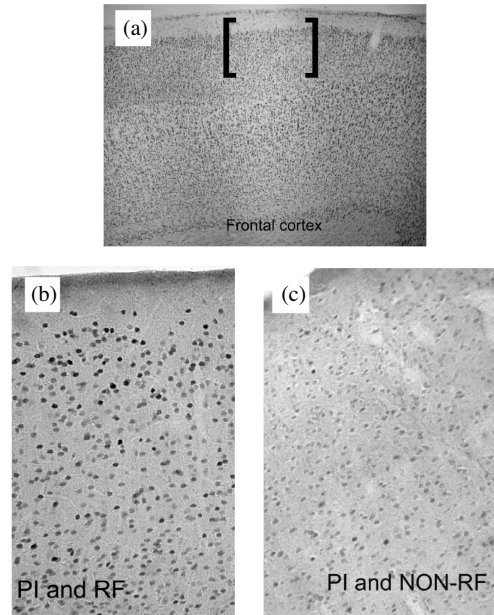


**Figure 7.** Photomicrographs of transverse sections through the frontal cortex of picrotoxin-treated rats. (a) Stained with toluidine blue, showing the size of the field used for c-Fos-positive neuron counting ( $\times [10X]$ ); (b) and (c) DAB-stained sections from irradiated (b) and non-irradiated (c) rats, showing c-Fos-positive neurons as DAB dots ( $\times [20X]$ ).

chamber. Rats that were not treated with picrotoxin (groups CR and CNR) initially showed stress (attributable largely to immobilization), but did not exhibit any abnormal activity or signs of seizure.

In both cortical areas of picrotoxin-treated rats, c-Fos-positive neurons appeared in all sections examined (Figure 7 shows sections of frontal cortex). Analysis of variance showed that both picrotoxin and radiation had statistically significant effects on c-Fos-positive neuron counts (hereinafter “counts”). In particular, in both cortical areas counts were about twice as high in group PR ( $133 \pm 7$  in frontal cortex,  $203 \pm 7$  in piriform cortex) as in group PNR ( $64 \pm 7$  in frontal cortex,  $110 \pm 8$  in piriform cortex) ( $p < 0.001$  in both areas), and more or less the same difference held between group CR and group CNR, although in this case the difference was only statistically significant in the piriform cortex ( $p < 0.003$ ) (see Figure 8).

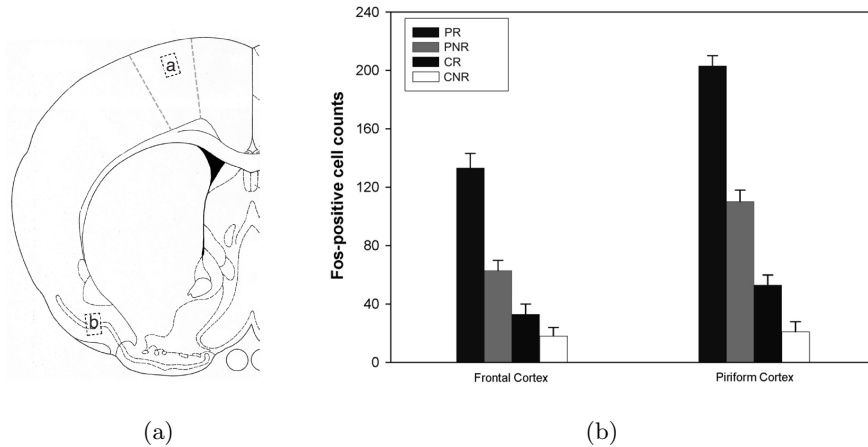


**Figure 8.** (a) Schematic drawing of a transverse section of the rat brain at the 9.2 mm level (interaural coordinates), showing the position of the frontal motor cortex (a) and piriform cortex (b). (b) c-Fos-positive neuron counts in the experimental groups (means of 7 or 8 rats, with SEMs shown as whiskers). PR, picrotoxin-treated rats irradiated with 1 W of 900 MHz GSM radiation; PNR, non-irradiated picrotoxin-treated rats; CR, irradiated control (non-picrotoxin-treated) rats; CNR, non-irradiated control rats.

#### 4. DISCUSSION

The experimental set-up described above allows controlled exposure of small laboratory animals to standing-wave RF radiation, measurement of the power absorbed by the experimental animal, and verification of the absence or negligibility of undesired (external) radiation and possible harmonics of the radiating system. The absorbed power measurement makes the determination of whole-body mean SAR trivial, and if the latter is assumed to be proportional to local SARs it can be used to adjust local SAR predictions obtained by simulation using a commercial FDTD program with a numerical phantom. As far as we know, this is the first time that standing waves have been used in studies of the biological effects of mobile communications radiation, in spite of their relevance to the use of mobile communications devices indoors [8].

There are two ways to estimate local SARs: by taking measurements of temperature [3, 4] or the electrical field [6], or by simulation using a numerical phantom [6, 7]. Measurements have the drawback of limited spatial precision, and that for brain and other vital

organs they can only be taken from dead animals, so that the degree to which they are really applicable to living tissues is questionable. As simulations are numeric-mathematical representations of real physical situations, they also have limitations, as far as they require general assumptions to be made about the electromagnetic characteristics of tissues. For application in studies using live animals, both methods require extrapolation of their findings from a dead or MR-imaged animal to the live experimental animal.

Hitherto, estimation of whole-body SARs has been based on the previous estimation of local SARs, and has therefore suffered from the uncertainties described above. The set-up described in this paper allows whole-body SAR to be determined directly from measurements of the weight of the live experimental animal and the power it absorbs. Furthermore, assuming local SARs to be proportional to whole-body SARs, the latter allows local SAR predictions based on simulations or on measurements in dead animals to be adjusted to the individual live experimental animal. In general, the correction made will be of about the same size as reported uncertainties in local SAR estimates obtained by measurement [4], simulation [1] or both [5].

The transcription factor *c-Fos* is a sensitive marker of neuronal activation [15]. In this study, *c-Fos*-positive neuron counts increased from group to group in the order  $CNR < CR < PNR < PR$  (Figure 8), both radiation and picrotoxin having statistically significant effects. As noted in the results section, the low estimated SARs imply that the effect of radiation cannot be attributed to hyperthermia, and nor can the differences between the effects of radiation on picrotoxin-treated and untreated rats be attributed to differences in power absorption. Neither the effect of picrotoxin nor the effect of radiation can be attributed to immobilization-induced stress [21], because all four experimental groups were immobilized for the same period.

The histological findings in the present study are virtually identical to those obtained previously [13], except that in the present study *c-Fos*-positive cell counts were higher in irradiated untreated rats (group CR) than in non-irradiated untreated rats (group CNR), the difference being statistically significant in the piriform cortex. The effect of radiation on *c-Fos*-positive cell counts in picrotoxin-treated rats is coherent with convulsions having been suffered by the irradiated rats (group PR) but not by the non-irradiated rats (group PNR); both findings suggest that 2 hours' exposure to 1 W GSM radiation markedly increased uncontrolled neuronal activity in the GABAergic and/or glutamatergic systems involving the frontal motor and piriform cortex [13, 22] following sensitization of these systems by subconvulsive doses of picrotoxin [14]. Despite of the fact that the experiments were

**Table 1.** Power absorbed by rats irradiated with 1 W of 900 MHz GSM radiation, with (group PR) or without (group CR) prior treatment with picrotoxin, together with rat weights and peak and mean SARs in brain and whole body (means of 8 rats in all cases). Whole-body mean SAR was calculated directly from the measured absorbed power, and other SARs using Equation (1).

Group	Absorbed power [mW]	Weight [g]	Estimated SARs [mW/g]			
			Whole-body mean SAR [mW/g]	Whole-body peak <sup>a</sup>	Mean in brain	Peak <sup>a</sup> in brain
PR	56.77	209.95	0.24	1.29	0.24	0.27
CR	60.28	211.83	0.25	1.37	0.26	0.29

<sup>a</sup>Maximum of the values obtained for 1g tissue elements by averaging over the element.

not performed with double blind design (as made with the c-Fos cells counts procedure, see Section 2.4), the experiments with the different rat groups were made on the same day time, therefore reducing the possibility of obtaining varying results due to stress levels (which are known to be different in the morning than in the evening, for example).

## 5. CONCLUSIONS

The simple set-up described in this paper allows controlled exposure of a small laboratory animal to standing-wave RF radiation and direct measurement of the power absorbed by the live animal (and hence of whole-body mean SAR, WBMSAR). Imprecision due to random errors in animal placement is estimated as at most about 36%. Assuming local SARs to be proportional to WBMSAR, the latter can then be used to adjust local SAR predictions obtained by simulation using a numerical phantom. The present illustrative study of the effects of 900 MHz GSM radiation on neural activity in rats made seizure-prone by subconvulsive doses of picrotoxin confirms our earlier finding that radiation doubles neural activity and is capable of triggering seizures in these animals even at very low SAR levels. Although the results of the work presented in this paper cannot be directly extrapolated to human beings, they should be taken as a warning about the possible effects of RF mobile telephone standing waves on humans with neuronal discharge susceptibility. This work can be considered as a stepping stone for a future research on that line.

## ACKNOWLEDGMENT

The authors thank the Secretariat General for Research and Development of the Xunta de Galicia for support under project PGIDIT02BFT20601PR, and Juan Vassal'lo, Jose Carlos Santos, Eva Domínguez, Eva García and Ian-Charles Coleman for advice and assistance of various kinds.

## REFERENCES

1. Kuster, N., V. Berdiñas Torres, N. Nikoloski, M. Frauscher, and W. Kainz, "Methodology of detailed dosimetry and treatment of uncertainty and variations for in vivo studies," *Bioelectromagnetics*, Vol. 27, 378–391, 2006.
2. Moros, E. G., W. L. Straube, and W. F. Pickard, "A compact shielded exposure system for the simultaneous long-term UHF irradiation of forty small mammals: I. Electromagnetic and environmental design," *Bioelectromagnetics*, Vol. 19, 459–468, 1998.
3. Swicord, M., J. Morrissey, D. Zakharia, M. Ballen, and Q. Balzano, "Dosimetry in mice exposed to 1.6 GHz microwave in a carousel irradiator," *Bioelectromagnetics*, Vol. 20, 42–27, 1999.
4. Moros, E. G., W. L. Straube, and W. F. Pickard, "Compact shielded exposure system for the simultaneous long-term UHF irradiation of forty small mammals: II. Dosimetry," *Bioelectromagnetics*, Vol. 20, 81–93, 1999.
5. Zygidis, T. T. and T. D. Tsiboukis, "Assessment of human head exposure to wireless communication devices: combined electromagnetic and thermal studies for diverse frequency bands," *Progress In Electromagnetics Research B*, Vol. 9, 83–96, 2008.
6. Schönborn, F., K. Pokovic, and N. Kuster, "Dosimetric analysis of the carousel setup for the exposure of rats at 1.62 GHz," *Bioelectromagnetics*, Vol. 25, 16–26, 2004.
7. Burkhardt, M., Y. Spinelli, and N. Kuster, "Exposure setup to test effects of wireless communications systems on the CNS," *Health and Physics*, Vol. 73, No. 5, 770–778, 1997.
8. Koester, P., J. Sakowski, W. Baumann, H. W. Glock, and J. Gimsa, "A new exposure system for the in vitro detection of GHz field effects on neuronal networks," *Bioelectrochemistry*, Vol. 70, No. 1, 104–114, Jan. 2007.
9. Hossmann, K. A. and D. M. Hermann, "Effects of electromagnetic

- radiation of mobile phones on the central nervous system,” *Bioelectromagnetics*, Vol. 24, 49–62, 2003.
10. Huber R., V. Treyer, J. Schuderer, T. Berthold, A. Buck, N. Kuster, H. P. Landolt, and P. Achermann, “Exposure to pulse-modulated radiofrequency electromagnetic fields affects regional cerebral blood flow,” *European Journal of Neuroscience*, Vol. 21, 1000–1009, 2005.
  11. Zhu, Y., F. Gao, X. Yang, H. Shen, and X. Liu, “The effect of microwave emission from mobile phones on neuron survival in rat central nervous system,” *Progress In Electromagnetics Research*, PIER 82, 287–298, 2008.
  12. Lin, J. C., “Cellular telephone radiation and electroencephalograms (EEG) of the human brain,” *IEEE Antennas and Propagation Magazine*, Vol. 45, No. 5, 150–153, 2003.
  13. Lopez-Martín, E., J. L. Relova-Quinteiro, R. Gallego-Gómez, M. Peleteiro-Fernández, F. J. Jorge-Barreiro, and F. J. Ares-Pena, “GSM radiation triggers seizures and increases cerebral c-Fos positivity in rats pretreated with subconvulsive doses of picrotoxin,” *Neuroscience Letters*, Vol. 298, 139–144, 2006.
  14. Nutt, D. J., P. J. Cowen, C. Batts, D. G. Grahame-Smith, and A. R. Green, “Repeated administration of subconvulsant doses of GABA antagonist drugs: I. Effect on seizure threshold (kindling),” *Psychopharmacology*, Vol. 76, 84–87, 1982.
  15. Morgan, J. I. and T. Curran, “Stimulus-transcription coupling in the nervous system: Involvement of the inducible proto-oncogenes fos and jun” *Annu. Rev. Neurosci.*, Vol. 14, 421–451, 1991.
  16. Willoughby, J. O., L. Mackenzi, A. Medvedev, and J. Hiscock, “Distribution of fos-positive neurons in cortical and subcortical structures after picrotoxin induced convulsions varies with seizure type,” *Brain Res.*, Vol. 683, 73–87, 1995.
  17. Schmid & Partner Engineering AG. 2006, “Reference manual for the SEMCAD simulation platform for electromagnetic compatibility, antenna design and dosimetry,” available from: <http://www.semcad.com>.
  18. Fritze, K., C. Wiessner, N. Kuster, C. Sommer, P. Gass, D. M. Hermann, M. Kiessling, and K. A. Hossmann, “Effects of GSM microwave exposure on the genomic response of the rat brain,” *Neuroscience*, Vol. 81, 627–639, 1997.
  19. Mickley, G. A., B. L. Cobb, P. A. Mason, and S. Farrell, “Disruption of a putative working memory task and selective expression of brain c-fos following microwave-induced hyperthermia,” *Physiol. Behav.*, Vol. 55, No. 6, 1029–1038, 1994.



20. Morrissey, R. W., S. Raney, E. Heasley, P. Rathinavelu, M. Dauphinee, and J. H. Fallon, "IRIDIUM exposure increases c-fos expression in the mouse brain only at levels which likely result in tissue heating," *Neuroscience*, Vol. 92, 1539–1546, 1999.
21. Cullinan, W. E., J. P. Herman, D. F. Battaglia, H. Akil, and S. J. Watson, "Pattern and time course of immediate early gene expression in rat brain following acute stress," *Neuroscience*, Vol. 64, No. 2, 477–505, 1995.
22. Mausset-Bonnefont, A. L., H. Hirbec, X. Bonnefont, A. Privat, J. Vignon, and R. de Seze, "Acute exposure to GSM 900-MHz electromagnetic fields induces glial reactivity and biochemical modifications in the rat brain," *Neurobiology of Disease*, Vol. 17, 445–454, 2004.